Sensors and Actuators B 150 (2010) 819–824

Contents lists available at ScienceDirect

Sensors and Actuators B: Chemical

journal homepage: www.elsevier.com/locate/snb

Fluidic device with pumping and sensing functions for precise flow control

Thien Xuan Dinh[a,*], Van Thanh Dau[a], Susumu Sugiyama[a], Phuc Hong Pham[b]

[a] *Ritsumeikan University, 1-1-1 Noji-Higashi, Kusatsu City, Shiga Prefecture 525-8577, Japan*
[b] *Hanoi University of Technology, 1-Dai Co Viet, Hai Ba Trung, Hanoi, Viet Nam*

ARTICLE INFO

Article history:
Received 5 February 2010
Received in revised form 15 July 2010
Accepted 9 August 2010
Available online 18 August 2010

Keywords:
Valveless micropump
Hotwire
Lab-on-a-chip
PZT diaphragm
MEMS

ABSTRACT

We have developed and characterized a planar fluidic device consisting of a piezoelectric (PZT) acutated valveless micropump and a p-type silicon hotwire as a flow sensor. The device is fabricated by standard MEMS process. The performance of the device is studied by experiment and simulation. The flow rate and backpressure attain 2.9 mL/min and 0.3 kPa, respectively, when using a 50 V_{p-p} sinusoidal driving voltage at the resonant frequency of 7.9 kHz. At low driving voltage of 10 V_{p-p} where the pump performance cannot be resolved by conventional flow meter, a flow rate of 0.05 mL/min is obtained by the hotwire. The successful integration of hotwire allows the device to be applicable to lab-on-a-chip analysis, gas sensing, and other systems where the integration and precise flow are required.

1. Introduction

The potential use of a lab-on-a-chip (LOC) requires integrating several elements such as valve, actuator, and sensor to manipulate fluid flow and to perform analysis on a single chip. The necessity of flow in LOC has enabled explosive research on micropump and other microfluidic components. Among the developed micropumps, valveless micropumps are a great interest since they avoid using any internal moving part. Flow in valveless micropumps can be conducted by the use of either non-mechanical or mechanical actuator [8]. Mechanical pumps actuated by piezoelectric (PZT) effect have been widely studied and fabricated, since they have simple structure, quick response and the actuator is available in commerce. In particular, PZT diaphragm has small stroke volume but large natural frequency and thus is suitable for gas pumping.

In literature, numerous principles and fabrication methods of micropump have been presented, but few of studies focused on their specific applications. Bourouina et al. [2] reported that their electrostatic micropump giving flow rate within 10–100 nl/min is suitable for drug delivery applications. Gan et al. [7] introduced an electroosmotic pump flow with large flow rate range (μl/min to mL/min) to determine chromium(VI) in wasted water. In bioengineering applications, an implantable micropump which is completely immersed within blood vessel for augmented liver perfusion is fabricated [10]. Usually, a LOC application requires controllable flow [13,4], and a micropump should be able to provide fluid with precise flow rate. Piezoelectric actuated micropumps can adjust its flow rate by alternating driving voltage and frequency with utilizing an external flow meter as a calibration tool. This typical method is not applicable for pumping a small flow rate because of the additional resistance of the flow meter. Furthermore, it makes the pump unable to integrate into a LOC system since the third party (i.e. flow meter) is required.

An alternative feasible approach is to integrate a “ready-used” calibrating element into micropumps such as hotwire anemometer which has been widely used in gas rate sensors [12,6,5]. In this paper, we develop a fluidic device consisting of a valveless micropump and a hotwire for self-measurement of flow rate. The device is fabricated by standard MEMS silicon process. The performance of the device is studied by both experiment and simulation. In addition, the high resolution flow measurement of the hotwire is demonstrated.

2. Design and working principle

The device is assembled from a fluidic network, two aluminum caps, and a PZT diaphragm as shown in Fig. 1(a). The fluidic network comprises a pump chamber, an outlet and two opposite inlet channels which are orthogonally connected together at the center of the pump. The cross-section of the outlet entrance is larger than that of the chamber nozzle but smaller than the cross section of the inlet nozzles (Fig. 1(b)). This structure creates proper fluidic resistance in the fluidic network and extracts Venturi’s effect at the center region to rectify the flow between pumping and suction phases; thus a net flow is produced from the inlet ports to outlet port. In this study, the cross-areas of the outlet entrance, cham-

---

* Corresponding author.
E-mail address: thien@cfd.ritsumei.ac.jp (T.X. Dinh).

0925-4005/$ – see front matter © 2010 Elsevier B.V. All rights reserved.
doi:10.1016/j.snb.2010.08.009

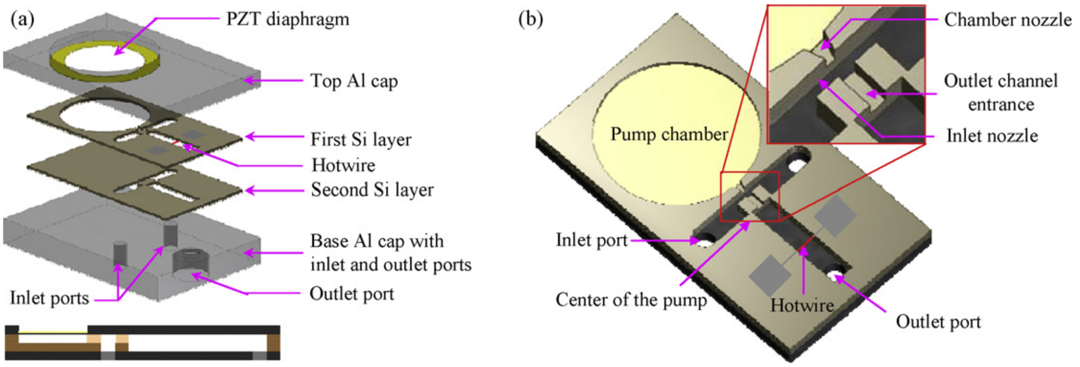

Fig. 1. The structure of the device (a) and the view of the device without the top cap (b).

ber nozzle, and inlet nozzles are designed as 0.5 mm × 0.5 mm, 0.5 mm × 0.3 mm, and 0.5 mm × 1 mm, respectively. The widths of inlet and outlet channels are 1.5 mm and diameter of the PZT diaphragm is 10 mm. A suspending hotwire with the dimension of 1000 μm × 10 μm × 5 μm ($L \times W \times T$) is integrated in the middle of the outlet channel at 2.5 mm in downstream from the center of the pump (Fig. 1).

3. Fabrication process

The fluidic network of the device is fabricated by standard MEMS process on two silicon layers: first layer including the hotwire is fabricated from silicon-on-insulator (SOI) wafer and second layer is fabricated from normal silicon wafer (Fig. 1(a)). A 500 μm p-type SOI wafer, device layer has 5 μm thickness and 0.3 Ω cm resistivity, is oxidized to form a 0.3 μm SiO_2 layer on both sides. The contact holes are opened through this insulator (Fig. 2(a)) and p+ is thermally diffused to improve doping concentration (Fig. 2(b)). The interconnecting wires with the thickness of 0.3 μm are made by vacuum evaporation, photolithography and aluminum etching. The Ohmic contact between the aluminum wires and device layer through the contact holes is achieved by thermal sintering at 450 °C (Fig. 2(c)). Hotwire is patterned by photolithography and etched by ICP-RIE on the device layer (Fig. 2(d)). In order to protect the thin-long structures from mechanical damages, the hotwires are successively covered by photoresist and polyimide (on front side). ICP-RIE is used again for backside etching (Fig. 2(e)) and the buried oxide is removed by RIE. The photoresist/polyimide protection layers are finally burned off by O_2 plasma asher (Fig. 2(f)). Second layer of the fluidic network is fabricated from 500 μm thick Si wafer by photolithography followed by a through-wafer ICP-RIE process.

First and second silicon layers are bonded together with epoxy so that the silicon hotwire is in the middle of them. Thermal treatment of the bonding process is performed for 30 min at 60 °C. Quality of the bonding is examined by digital microscope and we observed that the thickness of the epoxy layer is negligible in comparison with the depth of the fluidic network.

The pump chamber is closed by a PZT diaphragm inserted into the top cap and inlet and outlet ports are created through the base cap of the device. The schematic assembly of the device is shown in Fig. 2(g). Fig. 3 shows the fabricated fluidic network with the hotwire in the outlet channel. After packaging, the device is connected to an outer electric circuit by gold wire bonding as shown in Fig. 4.

4. Results and discussion

4.1. Pumping characteristic

To investigate the pumping performance of the device, the outlet port is connected to a soft tube and the inlet ports are set free. Flow rate is measured by M-200SCCM volume flow meter (Alicat Scientific Corporation) and backpressure is determined by KEYENCE Ap-44 pressure sensor (Keyence Corporation). Since the pressure sensor has low resolution, a display zero deadbank (ZDB) is set of 0.5% full scale (FS) below which the display simply jumps to zero to prevent the electrical noise.

The variation of the measured flow rate with frequency at the driving voltage $V_{PZT} = 50\,V$ is plotted in Fig. 5. It shows that the first

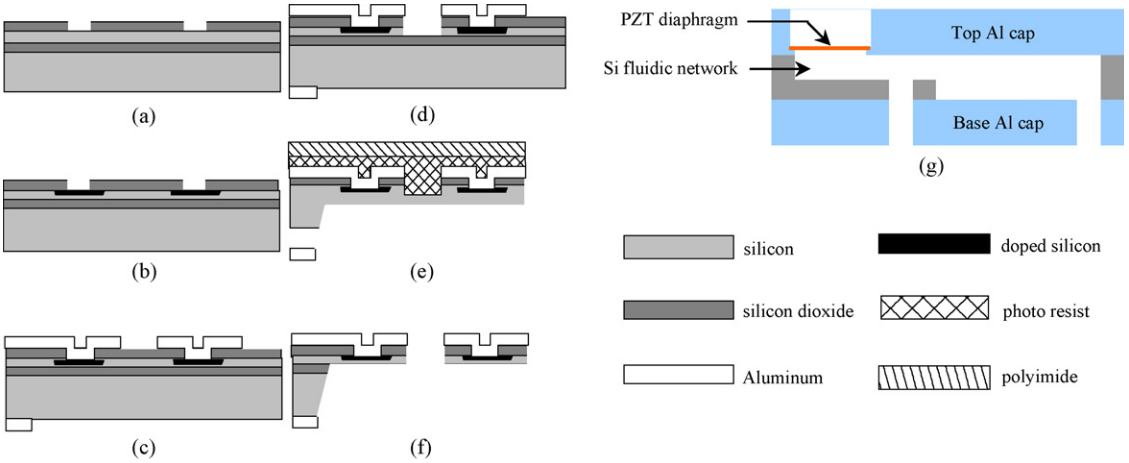

Fig. 2. The fabrication process of the fluidic network (a)–(f) and the assembled device (g).